The Monogenic Curvature Scale-Space*

Di Zang and Gerald Sommer

Cognitive Systems Group
Institute of Computer Science and Applied Mathematics
Christian Albrechts University of Kiel, 24118 Kiel, Germany
{zd,gs}@ks.informatik.uni-kiel.de

Abstract. In this paper, we address the topic of monogenic curvature scale-space. Combining methods of tensor algebra, monogenic signal and quadrature filter, the monogenic curvature signal, as a novel model for intrinsically two-dimensional (i2D) structures, is derived in an algebraically extended framework. It is unified with a scale concept by employing damped spherical harmonics as basis functions. This results in a monogenic curvature scale-space. Local amplitude, phase and orientation, as independent local features, are extracted. In contrast to the Gaussian curvature scale-space, our approach has the advantage of simultaneous estimation of local phase and orientation. The main contribution is the rotationally invariant phase estimation in the scale-space, which delivers access to various phase-based applications in computer vision.

1 Introduction

It is well know that corners and junctions play an important role in many computer vision tasks such as object recognition, motion estimation, image retrieval, see [1–4]. Consequently, signal modeling for such structures is of high significance. There are bulk of researches for intensity-based modeling, e.g. [5–7]. However, those approaches are not stable when the illumination varies. Phase information carries most essential structure information of the original signal [8]. It has the advantage of being invariant with respect to the illumination change. Hence, we intend to design a model for local structures with phase information contained. For 2D images, there are three types of structures, which can be associated with the term intrinsic dimension [7]. As a local property of multi-dimensional signals, it expresses the number of degrees of freedom necessary to describe local structures. The intrinsically zero dimensional (i0D) signals are constant signals. Intrinsically one dimensional (i1D) signals represent lines and edges. Corners, junctions, line ends, etc. are all intrinsically two dimensional (i2D) structures which have certain degrees of curvatures. There are lots of related work for 2D structures modeling. The structure tensor [5] estimates the main orientation and the energy of 2D structures. However, phase information is neglected. The Gaussian curvature scale-space [9, 10] enables the extraction of signal curvature in a

* This work was supported by German Research Association (DFG) Graduiertenkolleg No. 357 (DZ) and Grant So-320/2-3 (GS).

multi-scale way with no phase contained. A nonlinear curvature scale-space was proposed in [11] for shape representation and recognition, but it is impossible to extract phase information in this framework. Bülow and Sommer [12] proposed the quaternionic analytic signal, which enables the evaluation of the i2D signal phase. But it has the drawback of being not rotationally invariant. The monogenic signal [13] is a novel model for i1D signals. It is a generalization of the analytic signal in 2D and higher dimensions. However, the monogenic signal captures no information of the i2D part. A phase model is proposed in [14], where the i2D signal is split into two i1D signals and the corresponding two phases are evaluated. Unfortunately, steering is needed and only i2D patterns superimposed by two perpendicular i1D signals can be correctly handled.

In this paper, we present a novel approach to model i2D structures in a multi-scale way. Combining methods of tensor algebra, monogenic signal and quadrature filter, the monogenic curvature signal, as a novel model for i2D structures, is derived in an algebraically extended framework. It is unified with a scale concept by employing damped spherical harmonics as basis functions, which results in a monogenic curvature scale-space. Local amplitude, phase and orientation, as independent local features, are extracted. In contrast to the Gaussian curvature scale-space, our approach has the advantage of simultaneous estimation of local phase and orientation, which enables many phase-based applications in computer vision tasks.

2 Geometric Algebra Fundamentals

Geometric algebras [15–17] constitute a rich family of algebras as generalization of vector algebra. Compared with the classical framework of vector algebra, the geometric algebra enables a tremendous extension of modeling capabilities. By embedding our problem into a certain geometric algebra, more degrees of freedom can be obtained, which makes it possible to extract multiple features of i2D structures. For the problem we concentrate on, 2D image data is embedded into the Euclidean 3D space. Therefore, an overview of geometric algebra over Euclidean 3D space is given. The Euclidean space $\mathbb{R}^3$ is spanned by the orthonormal basis vectors $\{\mathbf{e}_1, \mathbf{e}_2, \mathbf{e}_3\}$. The geometric algebra $\mathbb{R}_3$ of the 3D Euclidean space consists of $2^3 = 8$ elements,

$$\mathbb{R}_3 = span\{1, \mathbf{e}_1, \mathbf{e}_2, \mathbf{e}_3, \mathbf{e}_{23}, \mathbf{e}_{31}, \mathbf{e}_{12}, \mathbf{e}_{123} = I_3\} \tag{1}$$

Here $\mathbf{e}_{23}$, $\mathbf{e}_{31}$ and $\mathbf{e}_{12}$ are the unit bivectors and the element $\mathbf{e}_{123}$ is a trivector or unit pseudoscalar. In this geometric algebra, vectors square to one, bivectors and trivector all square to minus one. A general combination of these elements is called a multivector

$$M = a + b\mathbf{e}_1 + c\mathbf{e}_2 + d\mathbf{e}_3 + e\mathbf{e}_{23} + f\mathbf{e}_{31} + g\mathbf{e}_{12} + hI_3 \tag{2}$$

The geometric product of two multivectors M_1 and M_2 is indicated by juxtaposition of M_1 and M_2, i.e. M_1M_2. The multiplication results of the basis elements are shown in table 1. The geometric product of two vectors $\mathbf{x} = x_1\mathbf{e}_1 + x_2\mathbf{e}_2$ and $\mathbf{y} = y_1\mathbf{e}_1 + y_2\mathbf{e}_2$ can be decomposed into their inner product $(\cdot)$ and outer product $(\wedge)$

$$\mathbf{x}\mathbf{y} = \mathbf{x} \cdot \mathbf{y} + \mathbf{x} \wedge \mathbf{y} \tag{3}$$

where the inner product of $\mathbf{x}$ and $\mathbf{y}$ is $\mathbf{x} \cdot \mathbf{y} = x_1y_1 + x_2y_2$ and the outer product is $\mathbf{x} \wedge \mathbf{y} = (x_1y_2 - x_2y_1)\mathbf{e}_{12}$.

Due to the orthogonality of basis vectors, their outer products are equivalent to their geometric products.

$$\mathbf{e}_1 \wedge \mathbf{e}_2 = \mathbf{e}_1\mathbf{e}_2 = \mathbf{e}_{12} \tag{4}$$

$$\mathbf{e}_2 \wedge \mathbf{e}_3 = \mathbf{e}_2\mathbf{e}_3 = \mathbf{e}_{23} \tag{5}$$

$$\mathbf{e}_3 \wedge \mathbf{e}_1 = \mathbf{e}_3\mathbf{e}_1 = \mathbf{e}_{31} \tag{6}$$

The k-grade part of a multivector is obtained from the grade operator $\langle M \rangle_k$. A blade of grade k, i.e. a k-blade B_k, is the outer product $(\wedge)$ of k independent vectors $\mathbf{x}_1, ..., \mathbf{x}_k \in \mathbb{R}^3$

$$B_k = \mathbf{x}_1 \wedge ... \wedge \mathbf{x}_k = \langle \mathbf{x}_1 ... \mathbf{x}_k \rangle_k \tag{7}$$

Hence, $\langle M \rangle_0$ is the scalar part of M, $\langle M \rangle_1$ represents the vector part, $\langle M \rangle_2$ indicates the bivector part and $\langle M \rangle_3$ is the trivector part, which commutes with every element of $\mathbb{R}_3$. The dual of a multivector M is defined to be the product

Table 1. The geometric product of basis elements.

	1	$\mathbf{e}_1$	$\mathbf{e}_2$	$\mathbf{e}_3$	$\mathbf{e}_{23}$	$\mathbf{e}_{31}$	$\mathbf{e}_{12}$	I_3
1	1	$\mathbf{e}_1$	$\mathbf{e}_2$	$\mathbf{e}_3$	$\mathbf{e}_{23}$	$\mathbf{e}_{31}$	$\mathbf{e}_{12}$	I_3
$\mathbf{e}_1$	$\mathbf{e}_1$	1	$\mathbf{e}_{12}$	$-\mathbf{e}_{31}$	I_3	$-\mathbf{e}_3$	$\mathbf{e}_2$	$\mathbf{e}_{23}$
$\mathbf{e}_2$	$\mathbf{e}_2$	$-\mathbf{e}_{12}$	1	$\mathbf{e}_{23}$	$\mathbf{e}_3$	I_3	$-\mathbf{e}_1$	$\mathbf{e}_{31}$
$\mathbf{e}_3$	$\mathbf{e}_3$	$\mathbf{e}_{31}$	$-\mathbf{e}_{23}$	1	$-\mathbf{e}_2$	$\mathbf{e}_1$	I_3	$\mathbf{e}_{12}$
$\mathbf{e}_{23}$	$\mathbf{e}_{23}$	I_3	$-\mathbf{e}_3$	$\mathbf{e}_2$	-1	$-\mathbf{e}_{12}$	$\mathbf{e}_{31}$	$-\mathbf{e}_1$
$\mathbf{e}_{31}$	$\mathbf{e}_{31}$	$\mathbf{e}_3$	I_3	$-\mathbf{e}_1$	$\mathbf{e}_{12}$	-1	$-\mathbf{e}_{23}$	$-\mathbf{e}_2$
$\mathbf{e}_{12}$	$\mathbf{e}_{12}$	$-\mathbf{e}_2$	$\mathbf{e}_1$	I_3	$-\mathbf{e}_{31}$	$\mathbf{e}_{23}$	-1	$-\mathbf{e}_3$
I_3	I_3	$\mathbf{e}_{23}$	$\mathbf{e}_{31}$	$\mathbf{e}_{12}$	$-\mathbf{e}_1$	$-\mathbf{e}_2$	$-\mathbf{e}_3$	-1

of M with the inverse of the unit pseudoscalar I_3

$$M^* = MI_3^{-1} = -MI_3 \tag{8}$$

The modulus of a multivector is obtained by $|M| = \sqrt{\langle M\widetilde{M} \rangle_0}$, where $\widetilde{M}$ is the reverse of a multivector defined as $\widetilde{M} = \langle M \rangle_0 + \langle M \rangle_1 - \langle M \rangle_2 - \langle M \rangle_3$.

If only the scalar and the bivectors are involved, the combined result is called a spinor

$$S = a + e\mathbf{e}_{23} + f\mathbf{e}_{31} + g\mathbf{e}_{12} \tag{9}$$

All spinors form a proper subalgebra of $\mathbb{R}_3$, that is the even subalgebra $\mathbb{R}_3^+$. A spinor represents a scaling-rotation, i.e. $S = r\exp(\theta B)$, where B is a bivector indicating the rotation plane, θ is the rotation angle within that plane and r refers to the scaling factor. It is shown in table 1 that the square of the bivector or trivector equals -1. Therefore, the imaginary unit i of the complex numbers can be substituted by a bivector or a trivector, yielding an algebra isomorphism. A vector-valued signal $\mathbf{f}$ in $\mathbb{R}_3$ can be considered as the result of a spinor acting on the $\mathbf{e}_3$ basis vector, i.e. $\mathbf{f} = b\mathbf{e}_1 + c\mathbf{e}_2 + d\mathbf{e}_3 = \mathbf{e}_3 S$. The transformation performed under the action of the spinor delivers access to both the amplitude and phase information of the vector-valued signal $\mathbf{f}$ [18]. From the logarithm of the spinor representation, two parts can be obtained. They are the scaling which corresponds to the local amplitude and the rotation which corresponds to the local phase representation. The $\mathbb{R}_3$-logarithm of a spinor $S \in \mathbb{R}_3^+$ takes the following form

$$\log(S) = \langle \log(S) \rangle_0 + \langle \log(S) \rangle_2 = \log(|S|) + \frac{\langle S \rangle_2}{|\langle S \rangle_2|} \mathrm{atan}\left(\frac{|\langle S \rangle_2|}{\langle S \rangle_0} \right) \tag{10}$$

where atan is the arc tangent mapping for the interval $[0, \pi)$. The scalar part $\langle \log(S) \rangle_0 = \log(|S|)$ illustrates the logarithm of the local amplitude, hence, local amplitude is obtained as the exponential of it

$$|S| = \exp(\log|S|) = \exp(\langle \log(S) \rangle_0) \tag{11}$$

The bivector part of $\log(S)$ indicates the local phase representation

$$\langle \log(S) \rangle_2 = \frac{\langle S \rangle_2}{|\langle S \rangle_2|} \mathrm{atan}\left(\frac{|\langle S \rangle_2|}{\langle S \rangle_0} \right) \tag{12}$$

3 Damped Spherical Harmonics

In the light of the proposal in [14], 2D damped spherical harmonics are employed as basis functions. Since we are more interested in the angular portions, the polar representation of damped spherical harmonics is used instead of the Cartesian form. Assume the angular behavior of a signal is band limited, therefore, only damped spherical harmonics from order zero to three are applied, otherwise, aliasing would occur. Damped spherical harmonics in the spectral domain have much simpler forms than that in the spatial domain. An nth order damped spherical harmonic in the Fourier domain reads

$$H_n = \exp(n\alpha\mathbf{e}_{12})\exp(-2\pi\rho s) = [\cos(n\alpha) + \sin(n\alpha)\mathbf{e}_{12}]\exp(-2\pi\rho s) \tag{13}$$

where n indicates the order of the damped spherical harmonic, ρ and α represent the polar coordinates, s is the scale parameter. The 2D damped spherical harmonics can be alternatively regarded as 2D spherical harmonics $\exp(n\alpha\mathbf{e}_{12})$ combined with a Poisson kernel $\exp(-2\pi\rho s)$ [19]. The Poisson kernel is a low-pass filter which, like the Gaussian kernel, will result in a linear scale-space, called Poisson scale-space. As a result, local signal analysis can be realized in a multi-scale approach. Except for the zero order, every damped spherical harmonic consists of two orthogonal components. In the spatial domain, damped spherical harmonics from order 0 to 3 are illustrated in Figure 1. The first order damped spherical harmonic H_1 is basically identical to the conjugate Poisson kernel [14]. When the scale parameter is set to zero, the conjugate Poisson kernel equals the Riesz transform [13].

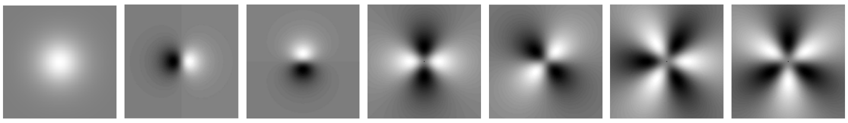

Fig. 1. From left to right are damped spherical harmonics from order 0 to 3 in the spatial domain (white:+1, black:-1). Except for zero order, every damped spherical harmonic consists of two orthogonal components.

4 The Monogenic Curvature Scale-Space

It is a well-known fact that 1D analytic functions correspond directly to 2D harmonic fields. In mathematics, these functions are also called holomorphic. Such functions are characterized by having a local power series expansion about each point [20]. This generalizes to 2D such that monogenic functions correspond to 3D harmonic fields. In Clifford analysis, the term monogenic is used to express the multidimensional character of the functions. Since in this paper, we present a novel approach which is to some degree a generalization of the analytic signal to the i2D case, it thus is called the monogenic extension of a curvature tensor. The monogenic curvature signal, as a novel model for i2D structures, can be derived from it. The monogenic scale-space, shown in Figure 2, is formed by the monogenic curvature signal at all scales.

4.1 Monogenic Extension of the Curvature Tensor

Motivated from the differential geometry, the curvature tensor can be constructed. Two dimensional intensity data can be represented as surfaces in 3D Euclidean space. Such surfaces in geometrical terms are Monge patches of the form

$$\mathbf{f} = \{x\mathbf{e}_1, y\mathbf{e}_2, f(x,y)\mathbf{e}_3\} \tag{14}$$

This representation makes it easy to use differential geometry to study the properties of the surface. The primary first-order differential quantity for an image is the gradient, which is defined as

$$\nabla \mathbf{f} = \sum_{i=1}^{2} g_i \mathbf{e}_i \frac{\partial \mathbf{f}}{\partial x_i} \tag{15}$$

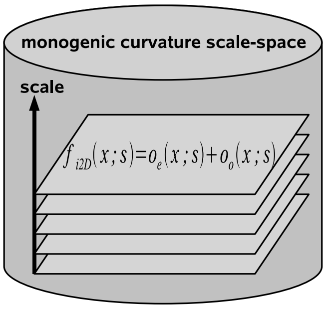

Fig. 2. The monogenic curvature scale-space.

where g_i indicates the following basis

$$g_1 = \begin{bmatrix} 1 \\ 0 \end{bmatrix} \quad g_2 = \begin{bmatrix} 0 \\ 1 \end{bmatrix} \tag{16}$$

Thereby, the gradient is reformulated as

$$\nabla \mathbf{f} = \begin{bmatrix} \mathbf{e}_1 \frac{\partial}{\partial x} f(x,y)\mathbf{e}_3 \\ \mathbf{e}_2 \frac{\partial}{\partial y} f(x,y)\mathbf{e}_3 \end{bmatrix} = \begin{bmatrix} f_x \mathbf{e}_{13} \\ f_y \mathbf{e}_{23} \end{bmatrix} \tag{17}$$

Analogously, as second-order differential quantity, the Hessian matrix H is given by

$$H = \begin{bmatrix} \mathbf{e}_1 \frac{\partial}{\partial x} f_x \mathbf{e}_{13} & \mathbf{e}_2 \frac{\partial}{\partial y} f_x \mathbf{e}_{13} \\ \mathbf{e}_1 \frac{\partial}{\partial x} f_y \mathbf{e}_{23} & \mathbf{e}_2 \frac{\partial}{\partial y} f_y \mathbf{e}_{23} \end{bmatrix} = \begin{bmatrix} f_{xx}\mathbf{e}_3 & -f_{xy}\mathbf{e}_{123} \\ f_{xy}\mathbf{e}_{123} & f_{yy}\mathbf{e}_3 \end{bmatrix} \tag{18}$$

This representation belongs to a hybrid matrix geometric algebra $M(2, \mathbb{R}_3)$, which is the geometric algebra of a 2×2 matrix with elements in $\mathbb{R}_3$, see [21].

According to the derivative theorem of Fourier theory [22], the Hessian matrix in the spectral domain reads

$$\mathcal{F}\{H\} = \begin{bmatrix} (-4\pi^2\rho^2 \frac{1+\cos(2\alpha)}{2}\mathbf{F}) & (4\pi^2\rho^2 \frac{\sin(2\alpha)}{2}\mathbf{F})\mathbf{e}_{12} \\ (-4\pi^2\rho^2 \frac{\sin(2\alpha)}{2}\mathbf{F})\mathbf{e}_{12} & (-4\pi^2\rho^2 \frac{1-\cos(2\alpha)}{2}\mathbf{F}) \end{bmatrix} \tag{19}$$

where $\mathcal{F}$ indicates the Fourier transform and $\mathbf{F}$ is the Fourier transform of the original signal $\mathbf{f}$. The angular parts of the derivatives are related to spherical harmonics of even order 0 and 2. It is well known that the Hessian matrix contains curvature information. Based on it, i0D, i1D and i2D signals can be separated by computing the trace and determinant. Therefore, we are motivated to construct a curvature tensor T_e, which is related to the Hessian matrix. The curvature tensor can be obtained from a tensor-valued filter, i.e. $T_e = \mathcal{F}^{-1}\{\mathbf{F}H_e\}$, where $\mathcal{F}^{-1}$ means the inverse Fourier transform and H_e indicates a tensor-valued filter in the frequency domain with the following form

$$H_e = \frac{1}{2}\begin{bmatrix} H_0 + \langle H_2\rangle_0 & -\langle H_2\rangle_2 \\ \langle H_2\rangle_2 & H_0 - \langle H_2\rangle_0 \end{bmatrix} = \frac{1}{2}\begin{bmatrix} 1+\cos(2\alpha) & -\sin(2\alpha)\mathbf{e}_{12} \\ \sin(2\alpha)\mathbf{e}_{12} & 1-\cos(2\alpha) \end{bmatrix}\exp(-2\pi\rho s)$$
$$= \begin{bmatrix} \cos^2(\alpha) & -\frac{1}{2}\sin(2\alpha)\mathbf{e}_{12} \\ \frac{1}{2}\sin(2\alpha)\mathbf{e}_{12} & \sin^2(\alpha) \end{bmatrix}\exp(-2\pi\rho s) \tag{20}$$

The angular portion of this filter is the same as that of the Hessian, according to equations (13) and (19), it is composed of even order 2D spherical harmonics H_0 and H_2. In this filter, components $\cos^2(\alpha)$ and $\sin^2(\alpha)$ are two angular windowing functions. They yield two perpendicular i1D components of the 2D image along the $\mathbf{e}_1$ and $\mathbf{e}_2$ coordinates. The other components of the filter are also the combination of two angular windowing functions, i.e. $\frac{1}{2}\sin(2\alpha) = \frac{1}{2}(\cos^2(\alpha - \frac{\pi}{4}) - \sin^2(\alpha - \frac{\pi}{4}))$. These two angular windowing functions result in two i1D components of the 2D image, which are oriented along the diagonals of the plane spanned by $\mathbf{e}_1$ and $\mathbf{e}_2$. All of the angular windowing functions are shown in Figure 3. They make sure that i1D components along different orientations are extracted. Consequently, this even filter enables the extraction of differently oriented even i1D components of the 2D image. Since the conjugate

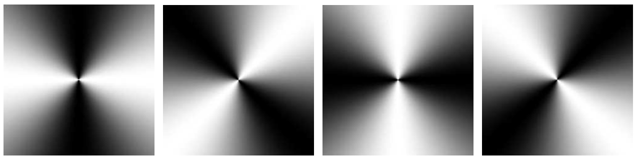

Fig. 3. From left to right are the angular windowing functions of $\cos^2(\alpha), \sin^2(\alpha - \frac{\pi}{4}), \sin^2(\alpha)$ and $\cos^2(\alpha - \frac{\pi}{4})$ with white:+1 and black:0.

Poisson kernel H_1 [14] is able to evaluate the corresponding odd information of the i1D signal, the odd representation of the curvature tensor is obtained by employing H_1 to its elements. Besides, the odd representation of the curvature tensor, denoted as T_o, can also result from a tensor-valued odd filter H_o, i.e. $T_o = h_1 * T_e = \mathcal{F}^{-1}\{H_o\mathbf{F}\}$ with h_1 referring to the spatial representation of the conjugate Poisson kernel. Thereby, the odd filter H_o can be obtained from the even filter by employing the conjugate Poisson kernel, i.e. $H_o = H_1 H_e$. In the spectral domain, the odd filter thus takes the following form

$$H_o = \frac{1}{2}\begin{bmatrix} H_1(H_0 + \langle H_2\rangle_0) & H_1(-\langle H_2\rangle_2) \\ H_1(\langle H_2\rangle_2) & H_1(H_0 - \langle H_2\rangle_0) \end{bmatrix} \tag{21}$$

Combing the curvature tensor and its odd representation forms a general 2D image representation, i.e. $T = T_e + T_o$. This algebraically extended representation can also be regarded as the monogenic extension of the curvature tensor.

4.2 The Monogenic Curvature Signal

Analogous with the differential geometry approach, 2D structures can be classified by computing the determinants and traces of the tensor pair T_e and T_o. Since the non-zero determinant indicates the existence of i2D structures, the even and odd parts of i2D structures are obtained from the determinants of the curvature tensor and its odd representation, respectively. The even part of i2D structures reads

$$o_e(\mathbf{x}; s) = \det(T_e)\mathbf{e}_3 = A\mathbf{e}_3 \tag{22}$$

The determinant of the curvature tensor is scalar valued. Therefore, same as the monogenic signal, the even part of i2D structures is embedded as the $\mathbf{e}_3$ component in the 3D Euclidean space. The odd part of i2D structures is

$$o_o(\mathbf{x}; s) = \det(T_o)\mathbf{e}_2 = B\mathbf{e}_1 + C\mathbf{e}_2 \tag{23}$$

Because $\det(T_o)$ is spinor valued, by multiplying the $\mathbf{e}_2$ basis from the right, $o_o(\mathbf{x}; s)$ takes a vector valued representation. Hence, a local representation for i2D structures is obtained by combining the even and odd parts of i2D structures. This local representation for i2D structures is called the monogenic curvature signal and it takes the following form

$$\mathbf{f}_{i2D}(\mathbf{x}; s) = o_e(\mathbf{x}; s) + o_o(\mathbf{x}; s) = A\mathbf{e}_3 + B\mathbf{e}_1 + C\mathbf{e}_2 \tag{24}$$

The original scalar signal $f(\mathbf{x}), \mathbf{x} \in \mathbb{R}^2$ is thus mapped to a vector-valued signal $\mathbf{f}_{i2D}(\mathbf{x}; s)$ in $\mathbb{R}_3$ as a local representation of i2D signals.

4.3 Local Features and Geometric Model

According to the introduction in Section 2, local features of the monogenic curvature signal can be defined using the logarithm of $\mathbb{R}_3^+$. The spinor field which maps the $\mathbf{e}_3$ basis vector to the monogenic curvature signal $\mathbf{f}_{i2D}(\mathbf{x}; s)$ is given by $\mathbf{f}_{i2D}(\mathbf{x}; s)\mathbf{e}_3$. The local amplitude and local phase representation are obtained as

$$|\mathbf{f}_{i2D}(\mathbf{x}; s)| = \exp(\langle \log(\mathbf{f}_{i2D}(\mathbf{x}; s)\mathbf{e}_3)\rangle_0) = \exp(\log(|\mathbf{f}_{i2D}(\mathbf{x}; s)\mathbf{e}_3|)) \tag{25}$$

$$\arg(\mathbf{f}_{i2D}(\mathbf{x}; s)) = \frac{\langle \mathbf{f}_{i2D}(\mathbf{x}; s)\mathbf{e}_3\rangle_2}{|\langle \mathbf{f}_{i2D}(\mathbf{x}; s)\mathbf{e}_3\rangle_2|} \operatorname{atan}\left(\frac{|\langle \mathbf{f}_{i2D}(\mathbf{x}; s)\mathbf{e}_3\rangle_2|}{\langle \mathbf{f}_{i2D}(\mathbf{x}; s)\mathbf{e}_3\rangle_0}\right) \tag{26}$$

where $\arctan(\cdot) \in [0, \pi)$ and $\arg(\cdot)$ denotes the argument of the expression. As the bivector part of the logarithm of the spinor field $\mathbf{f}_{i2D}(\mathbf{x}; s)\mathbf{e}_3$, this local phase representation describes a rotation from the $\mathbf{e}_3$ axis by a phase angle φ in the oriented complex plane spanned by $\mathbf{f}_{i2D}(\mathbf{x}; s)$ and $\mathbf{e}_3$, i.e. $\mathbf{f}_{i2D}(\mathbf{x}; s) \wedge \mathbf{e}_3$. The orientation of this complex plane indicates the local main orientation. Therefore, the local phase representation combines local phase and local orientation of i2D structures. The dual of the complex plane $\mathbf{f}_{i2D}(\mathbf{x}; s) \wedge \mathbf{e}_3$ is a rotation vector

$$\mathbf{r}(\mathbf{x}; s) = (\arg(\mathbf{f}_{i2D}(\mathbf{x}; s)))^* = \langle \log(\mathbf{f}_{i2D}(\mathbf{x}; s)\mathbf{e}_3)\rangle_2^* \tag{27}$$

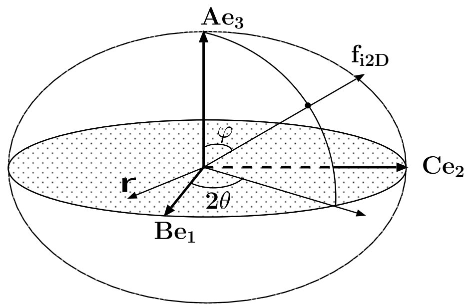

Fig. 4. The geometric model for the monogenic curvature signal. Here, φ is the phase, 2θ denotes the main orientation in terms of double angle representation, $\mathbf{r}$ indicates the rotation vector.

The rotation vector $\mathbf{r}(\mathbf{x}; s)$ is orthogonal to the local orientation and its absolute value represents the phase angle of the i2D structure. With the algebraic embedding, a geometric model for the monogenic curvature signal can be visualized as is shown in Figure 4. The geometric model is an ellipsoid, which looks very similar to that of the monogenic signal. However, each axis encodes totally different meaning. The even part of the i2D structure is encoded within the $\mathbf{e}_3$ axis, and the odd information is encoded within the plane spanned by $\mathbf{e}_1$ and $\mathbf{e}_2$ axes. The angle φ represents the phase and 2θ is the main orientation in a double angle representation form. The rotation vector $\mathbf{r}$ lies in the plane orthogonal to $\mathbf{e}_3$ since it is dual to the bivector $\mathbf{f}_{i2D} \wedge \mathbf{e}_3$. Combining the local amplitude and local phase representation, the monogenic curvature signal for i2D structures, can be reconstructed as

$$\mathbf{f}_{i2D} = |\mathbf{f}_{i2D}| \exp\left(\arg\left(\mathbf{f}_{i2D}\right)\right) \tag{28}$$

Having a definition for the i2D local features, we recognize that local amplitude, phase and orientation are scale dependent. However, they are independent of each other at each scale.

Gaussian curvature scale-space [9, 10] and the morphological curvature scale-space [11] are suitable for recovering invariant geometric features of a signal at multiple scales. However, the definition of curvatures and the scale generating operator are totally different from our approach. Besides, no phase information is contained in those frameworks. In contrast to these methods, our approach enables the simultaneous estimation of local amplitude, local phase and orientation information in a common scale-space concept. Consequently, the monogenic curvature scale-space has a unique advantage if a quadrature relationship concept is required.

5 Experimental Results

In this section, we show some experimental results in the framework of the monogenic curvature scale-space. A synthetic image superimposed by an angular and a radial modulation is adopted as the test image. The blobs in this image are regarded as i2D structures. The monogenic curvature signal at a certain scale can be obtained to characterize i2D structures. The test image and extracted local features are illustrated in Figure 5.

The estimated orientation denotes the continuous main orientation at a certain scale. Because the evaluated orientation has a value between 0 and π, it is wrapped along the horizontal axis. The local energy output, i.e. square of the local amplitude, indicates the existence of i2D structures. Besides, it also demonstrates the rotation-invariant property of the monogenic curvature signal. Local energy outputs of the test image at three different scales are shown.

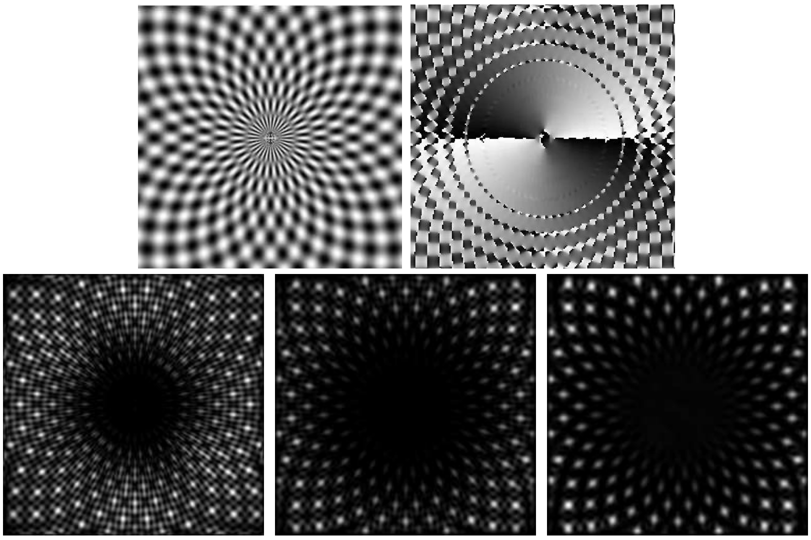

Fig. 5. Top row: from left to right are the test image and the orientation estimation at a certain scale of the monogenic curvature scale-space. Bottom row: local energy outputs at three different scales.

Another test image is composed of two cosine signals with different frequencies, amplitudes and orientations. The test image and the estimated phase information are shown in Figure 6. Because the local amplitude and local phase are independent of each other, when the illumination of the original image varies, the estimated local phase is still stable. This delivers access to many phase-based processing techniques in computer vision.

The monogenic curvature signal is a novel model for i2D structures, which handles the type of structure that the monogenic signal cannot correctly deal with. The third experiment aims to show the difference of these two models. Figure 7 demonstrates local energies and local phases extracted from the monogenic signal and the monogenic curvature signal. It is obvious that the monogenic

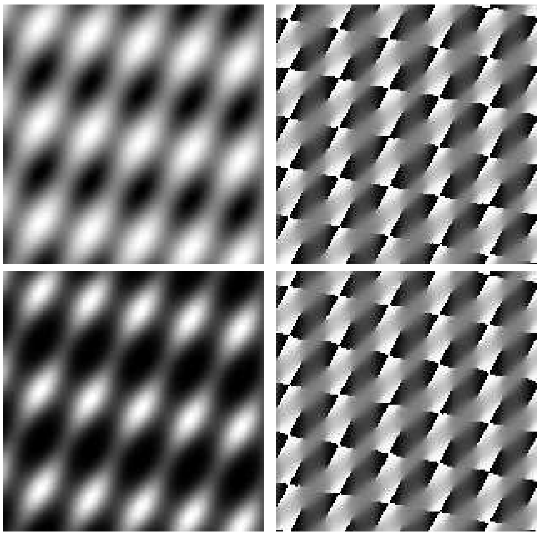

Fig. 6. Top row: from left to right are the test image and its phase estimation. Bottom row: the illumination changed test image and its phase evaluation.

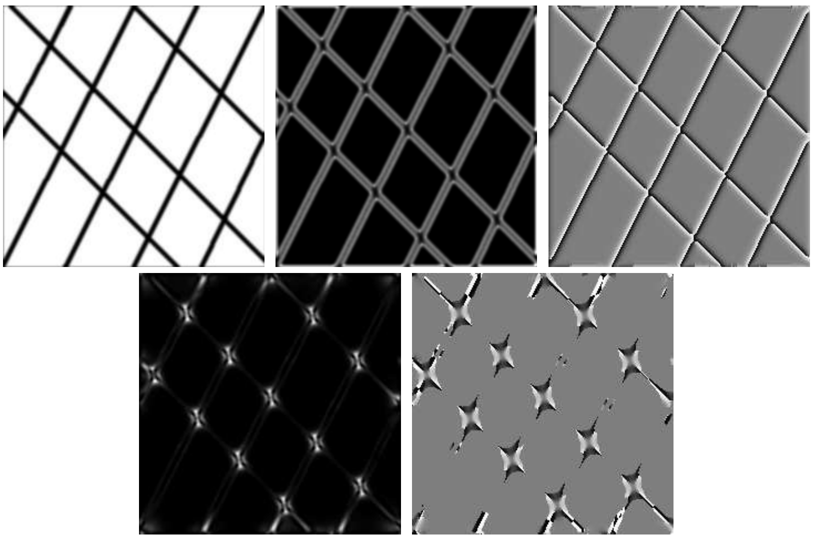

Fig. 7. Top row: test image, the energy of the monogenic signal and its phase. Bottom row: Energy and phase of the monogenic curvature signal.

signal responds to i1D structures and the monogenic curvature signal extracts features from i2D structures.

6 Conclusions

We present the monogenic curvature scale-space in this paper. Coupling methods of tensor algebra, monogenic signal and quadrature filter, the monogenic curvature signal, which characterizes i2D structures is obtained. Employing damped spherical harmonics as basis functions unifies a scale concept with the monogenic curvature signal. The monogenic curvatures scale-space is thus formed by the monogenic curvature signals at all scales. Local amplitude, local phase and local orientation of i2D structures, as independent features, can be extracted. Compared with the Gaussian curvature scale-space and the morphological curvature scale-space, our approach has remarkable advantage of simultaneous estimation of local phase and local orientation, which delivers access to various applications in the computer vision.

References

1. Costabile, M.F., Guerra, C., Pieroni, G.G.: Matching shapes: a case study in time varying images. Computer Vision, Graphics and Image Processing **29** (1985) 296–310
2. Han, M.H., Jang, D.: The use of maximum curvature points for the recognition of partially occluded objects. Pattern Recognition **23** (1990) 21–33
3. Liu, H.C., Srinath, M.D.: Partial classification using contour matching in distance transformation. IEEE Transactions on Pattern Analysis and Matchine Intelligence **12** (1990) 1072–1079
4. Wang, H., Brady, M.: Real-time corner detection algorithm for motion estimation. Image and Vision Computing **13** (1995) 695–703
5. Förstner, W., Gülch, E.: A fast operator for detection and precise location of distinct points, corners and centers of circular features. In: Proc. ISPRS Intercommission Conference on Fast Processing of Photogrammetric Data, Interlaken, Switzerland (1987) 281–305
6. Köthe, U.: Integrated edge and junction detection with the boundary tensor. In: Proceeding of 9th Intl. Conf. on Computer Vision. Volume 1. (2003) 424–431
7. Krieger, G., Zetzsche, C.: Nonlinear image operators for the evaluation of local intrinsic dimensionality. IEEE Transactions on Image Processing **5** (1996)
8. Oppenheim, A.V., Lim, J.S.: The importance of phase in signals. IEEE Proceedings **69** (1981) 529–541
9. Mokhtarian, F., Suomela, R.: Curvature scale space for robust image corner detection. In: Proc. 14th International Conference on Pattern Recognition (ICPR'98). Volume 2. (1998) 1819–1821
10. Mokhtarian, F., Bober, M.: Curvature scale space representation: theory, applications, and MPEG-7 standardization. Kluwer Academic Publishers (2003)
11. Jalba, A.C., Wilkinson, M.H.F., Roerdink, J.B.T.M.: Shape representation and recognition through morphological curvature scale spaces. IEEE Trans. Image Processing **15** (2006) 331–341

12. Bülow, T., Sommer, G.: Hypercomplex signals - a novel extension of the analytic signal to the multidimensional case. IEEE Transactions on Signal Processing **49** (2001) 2844–2852
13. Felsberg, M., Sommer, G.: The monogenic signal. IEEE Transactions on Signal Processing **49** (2001) 3136–3144
14. Felsberg, M.: Low-level image processing with the structure multivector. Technical Report 2016, Christian-Albrechts-Universität zu Kiel, Institut für Informatik und Praktische Mathematik (2002)
15. Lounesto, P.: Clifford Algebras and Spinors. Cambridge University Press (1997)
16. Ablamowicz, R.: Clifford Algebras with Numeric and Symbolic Computations. Birkhäuser, Boston (1996)
17. Hestenes, D., Li, H., Rockwood, A.: Geometric computing with clifford algebras. In Sommer, G., ed.: New Algebraic Tools for Classical Geometry. Springer-Verlag (2001) 3–23
18. Sommer, G., Zang, D.: Parity symmetry in multi-dimensional signals. In: Proc. of the 4th International Conference on Wavelet Analysis and its Applications, Macao (2005)
19. Felsberg, M., Sommer, G.: The monogenic scale-space: A unifying approach to phase-based image processing in scale-space. Journal of Mathematical Imaging and Vision **21** (2004) 5–26
20. Stein, E., Weiss, G.: Introduction to Fourier Analysis on Euclidean Spaces. Princeton University Press, New Jersey (1971)
21. Sobczyk, G., Erlebacher, G.: Hybrid matrix geometric algebra. In Li, H., Olver, P.J., Sommer, G., eds.: Computer Algebra and Geometric Algebra with Applications. Volume 3519 of LNCS., Springer-Verlag, Berlin Heidelberg (2005) 191–206
22. Bracewell, R.: Fourier Analysis and Imaging. Kluwer Academic / Plenum Publishers, New York (2003)